DOI: 10.61782/fa.2025.0169

FORUM ACUSTICUM
EURONOISE 2025

BAYESIAN ANALYSIS OF THE RW BASED ON A PARAMETRIZED PHYSICAL MODEL ACCORDING TO EN ISO 12354-1

Michael Parzinger[1*] **Ulrich Schanda**[1]
[1] Laboratory for Sound Measurement, Technical University of Applied Sciences Rosenheim, Germany

ABSTRACT

The EN ISO 12354-1 standard provides a physical model for the sound reduction index R. The results of this model can be used to calculate the weighted sound reduction index for different scenarios, which itself plays an important role in the design of a building element. This raises the question of how well this physical model actually reflects reality. In this work, the physical model is first optimized based on Bayesian inference. The optimized model can then in turn be used to simulate the sound reduction index taking into account uncertainties. These simulations then can provide an analysis of the construction in order to decide whether the minimum requirements on sound insulation will be met with a certain probability. For example, it is checked how thick a calcium silicate brick wall must be so that the weighted sound reduction index is at least 53 dB with a probability of 95 %. This is relevant as, in the best-case scenario, building elements can be optimized concerning the economization of material, which enables a cost-effective and sustainable construction.

Keywords: *Sound reduction index, Rw, Bayesian inference*

1. INTRODUCTION

For new buildings, an optimized construction in terms of sustainability is compulsory. Requirements on sound insulation have to be met as well. Often, the question arises as to how thick a solid wall should be. Thin walls would save material, whereas thick walls guarantee better sound insulation. This paper focuses on the influence of the thickness of a homogeneous wall on the weighted sound reduction index R_w using a Bayesian approach.

To investigate this issue, a physical model for the sound reduction index R is considered. This physical model is first optimized using data from laboratory measurements of walls made of calcium silicate (Ca-Si) blocks. This part was also discussed at Forum Acusticum 2023 [1] and at [2, 3], but has been expanded since then.

With this optimized model, the sound reduction index is simulated by drawing realizations from a corresponding probability distribution. The values for the weighted sound reduction index can then be calculated and analyzed. This procedure is finally used for claims about wall thicknesses that do not occur in the available data. In particular, the probability of whether a wall meets a certain requirement on the weighted sound reduction index is estimated.

2. PHYSICAL MODEL

First, a physical model for the sound reduction index R is discussed, which is based on the model in ISO 12354-1 Annex B [4] and given in equation (1). A few modifications have been implemented and are explained in DAS/DAGA [5]. All quantities in the following equations together with the chosen numerical values are listed in Table 1. The second term in equation (1) denotes the Waterhouse correction.

$$R = -10\lg(\tau) - 10\lg\left(1 + \frac{c_0 S_\mathrm{tot}}{8Vf}\right) \qquad (1)$$

The transmission coefficient in the first term is given

*Corresponding author: Michael.Parzinger@TH-Rosenheim.de.

in equation (2), while the radiation factor σ is defined by the equation (6).

$$\tau = \begin{cases} \frac{Z_0^2}{(m'\pi f)^2}\left(\frac{\pi}{2}\frac{\sigma^2}{\eta_{\text{tot}}}\frac{f_c}{f} + \frac{2\sigma_f}{(1-f^2/f_c^2)^2}\right), & f < 0.89 f_c \\ \frac{Z_0^2}{(m'\pi f)^2}\frac{\pi}{2}\frac{\sigma^2}{\eta_{\text{tot}}}, & 0.89 f_c \leq f \leq 1.4 f_c \\ \frac{Z_0^2}{(m'\pi f)^2}\frac{\pi}{2}\frac{\sigma^2}{\eta_{\text{tot}}}\frac{f_{c,\text{eff}}}{f}, & f > 1.4 f_c \end{cases} \tag{2}$$

$$f_c = \frac{\sqrt{3}}{\pi}\frac{c_0^2}{c_{\text{L}}}\frac{1}{t} \tag{3}$$

$$f_{\text{c,eff}} = f_{\text{c}} \cdot \left(1 + \frac{1}{\gamma^3} \cdot \left(\frac{3.6}{1-\mu} \cdot \frac{tf}{c_{\text{L}}}\right)^{\frac{3}{2}}\right)^{\frac{2}{3}} \tag{4}$$

$$\eta_{\text{tot}} = \eta_{\text{int}} + \text{C}/\sqrt{f} \tag{5}$$

The calculations of the radiation factor are strongly based on ISO 12354-1, only the maximum value is adjusted due to ambiguities in the standard and because past analyses have shown that these adjustments are appropriate.

$$\sigma(f) = \min\left(\tilde{\sigma}(f); \sigma_3(f); \sqrt{1 + \frac{2(l_1+l_2)\cdot f_{\text{c}}}{5c_0}}; 2.0\right) \tag{6}$$

Further adjustments have been made in the high frequency range, where thickness resonances occur. For this purpose, a new quantity τ_0 is introduced in equation (7). The definition of c_{L1} signifies that in this work a distinction is made between the effective value c_{L} and the nominal (material) value c_{L1} for the longitudinal wave velocity.

$$\tau_0 = \left(\cos^2(u) + \frac{1}{4}\left(\frac{\rho c_{\text{L,ex}}}{Z_0} + \frac{Z_0}{\rho c_{\text{L,ex}}}\right)^2 \sin^2(u) + \eta_{\text{int}}^2\right)^{-1} \tag{7}$$

$$u = \frac{2\pi f t}{c_{\text{L,ex}}} \tag{8}$$

$$c_{\text{L,ex}} = c_{\text{L1}}\frac{1-\mu}{\sqrt{1-2\mu}} \tag{9}$$

The following variables are introduced:

$$f_{\text{T}} = \sqrt{3}(1-\mu)\frac{c_{\text{L1}}}{2\pi t} \tag{10}$$

$$\tilde{f}_{\text{T}} = \arg\min_f |\log(f) - \log(2^{2/3} f_{\text{T}})| \tag{11}$$

$$\tau_{\text{plateau}} = \frac{\eta_{\text{ref}}}{\eta_{\text{tot}}}\left(\frac{4Z_0}{\rho c_{\text{L,ex}}}\right)^2 \tag{12}$$

$$\eta_{\text{ref}} = \eta_{\text{int}} + \frac{\text{C}}{\sqrt{2^{2/3} f_{\text{T}}}} \tag{13}$$

$$\tau_{\text{w}}(f) = (\tau_{\text{plateau}}(f)^4 \tau_0(f))^{1/5} \tag{14}$$

Finally, the adjusted transmission coefficient is defined in equation (15).

$$\tau_{\text{adj}}(f) = \begin{cases} \tau(f), & f \leq \tilde{f}_{\text{T}} \\ \tau_{\text{w}}(f) \cdot \tau(\tilde{f}_{\text{T}})/\tau_{\text{w}}(\tilde{f}_{\text{T}}), & f > \tilde{f}_{\text{T}} \end{cases} \tag{15}$$

Table 1. Quantities for the sound reduction index R.

Symbol	Description	Value
f	Frequency in Hz	
c_0	Sound speed in air	340 m/s
S_{tot}	Total surface in reception room	85 m²
V	Reception room volume	50 m³
Z_0	Sound characteristic impedance of air	418 $\frac{Pa}{m/s}$
m’	Mass per unit area	440 kg/m²
σ_f	Radiation factor for forced waves	See ISO 12354-1
$\tilde{\sigma}$	Radiation factor	See ISO 12354-1
σ_3	-	See ISO 12354-1
ρ	Density of the material	1760 kg/m³
μ	Poisson’s ratio	0.25
t	Construction thickness	0.25 m
l_1, l_2	Side lengths of wall	Depends
c_{L1}	Nominal longitudinal wave velocity	2500 m/s
c_{L}	Effective longitudinal wave velocity	Fit parameter
C	Boundary loss constant	Fit parameter
η_{int}	Internal loss factor	Fit parameter
γ	Shear wave contribution factor	Fit parameter

3. DATA DESCRIPTION

For the next step, data from 24 laboratory measurements will be used to further customize the model. These originate from a round robin test carried out by the *Physikalisch-Technische Bundesanstalt* (PTB). The separating components are Ca-Si walls with a thickness of 25 cm including plaster. Further details on the laboratory experiments can be found in [6] and [7]. Figure 1 shows the mean progression of these 24 curves and the range resulting from the mean value ± 1 respectively ± 2 times the standard deviation of the measurement data.

4. BAYESIAN INFERENCE

The data is now the basis for the optimization of the physical model from section 2 by only changing some parameters but not the physics of the model. Bayesian methods are applied for this purpose. The Bayesian concept of probability is characterized by the idea that probabilities are not interpreted as relative frequencies but as degrees of belief that can be updated with new information. For the application, a distribution is assumed which represents the knowledge of our parameter before the data is known. This distribution is referred to as the prior distribution. The data y is then combined with the prior distribution to obtain a posterior distribution. This posterior distribution represents the knowledge of the parameter after the data is taken into account. Since the knowledge is expressed by probability distributions, it also contains all uncertainties of the parameters. To derive this posterior, Bayes' theorem from equation (16) is applied (s. subsection 4.1). The term $\propto$ denotes equality except for factors that do not depend on θ. The concept of Bayesian statistics is further discussed in several books like [8], [9], and [10].

$$\underbrace{\mathbf{p}(\theta|y)}_{\text{posterior}} = \frac{\mathbf{p}(\theta)\,\mathbf{p}(\theta|y)}{\mathbf{p}(y)} \propto \underbrace{\mathbf{p}(\theta)}_{\text{prior}}\,\underbrace{\mathbf{p}(y|\theta)}_{\text{likelihood}} \tag{16}$$

On the one hand, this approach is suitable when there are few data relative to the number of parameters to be estimated. This is because sample size plays a less central role in Bayesian statistics than in classical statistics. On the other hand, some of the parameters are physical quantities for which prior knowledge exists. The term $\mathbf{p}(\theta)\,\mathbf{p}(y|\theta)$ can also be interpreted in such a way that the parameters are pushed away from the data optimum in the direction of physically meaningful values.

This is also the difference to the classical approach, also known as the frequentist approach, in which θ is chosen such that it maximizes the likelihood $\mathbf{p}(y|\theta)$. The analysis using the classic approach was presented at this year's DAS/DAGA [5].

4.1 Definitions and assumptions

First, the physical parameters to be adjusted are selected. These are the internal loss factor η_{int}, the boundary loss constant C, the longitudinal wave velocity c_{L} of the plate, and γ. Therefore, $\phi = (\eta_{\text{int}}, \text{C}, c_{\text{L}}, \gamma)^T \in \mathbb{R}^4$ is defined as the vector of physical fit parameters.

In addition to these, a covariance matrix is also necessary, which is defined as $\Sigma \in \mathbb{R}^{21\times 21}$ and indicates the third-octave band-dependent variances on the diagonal and the covariances between two third-octave bands outside of it. For this purpose, $\theta = (\phi, \Sigma)$ is denoted as the tuple of ϕ and Σ.

The measurement curves are each denoted as y_i with $i = 1, \ldots, 24$. A multidimensional normal distribution is assumed for these if ϕ and Σ are given, i.e. $y_i|\theta \sim \mathcal{N}_{21}(\text{M}_i(\phi), \Sigma)$. Here, $\text{M}_i : \mathbb{R}^4 \to \mathbb{R}^{21}$ denotes the physical model as a function of the physical fit parameters. This results in a potential model curve for each ϕ. The index in M_i indicates that the properties of the i-th wall are taken into account. This refers in particular to the side lengths.

The notation y in equation (16) represents the vector of all 24 measurement curves, i.e. $y = (y_1^T, y_2^T, \ldots, y_{24}^T)^T \in \mathbb{R}^{504}$, where $504 = 21 \cdot 24$ results from the number of third octave bands times the number of measurement curves. It is assumed that the measurement curves are independent of each other.

4.2 Prior distributions

Maximum Entropy Prior (MEP) is applied to convert physical prior knowledge into a prior distribution. The MEP was introduced by Jaynes [11, 12] and further discussed in [13], [14], [15] and others.

If prior knowledge of the expected value, variance, minimum, and maximum is available for a one-dimensional parameter, then the truncated normal distribution results as the prior distribution [15, Page 201].

The prior assumptions for the physical fit parameters ϕ are shown in Table 2. Note that for the longitudinal velocity c_{L} the effective value and not the nominal value is meant. These assumptions are based on individual experience, but this only plays a minor role for the results as long as other prior knowledge does not deviate too much from the Table 2 values.

Table 2. Prior assumptions for the parameters ϕ

Parameter	Mean	Variance	Min.	Max.
η_{int}	0.02	0.01^2	0.005	∞
C	2	1	0.25	5
c_L in m/s	1000	300^2	700	5000
γ	0.77	0.2^2	0.55	0.95

Both the variances and the correlations are required for the prior distribution of the covariance matrix. The variances are based on the work of Wittstock (2015) [16]. With MEP, this results in the exponential distribution with the calculated average as the expected value for each one-third octave band.

The LKJ (Lewandowski, Kurowicka, Joe) [17] distribution is employed to model prior knowledge about correlations. This distribution is given by $\mathbf{p}(\Omega|\nu) \propto |\Omega|^{\nu-1}$ for each correlation matrix Ω. The parameter ν represents the prior knowledge about the correlation. If ν is less than one, high correlations are assumed; if ν is greater than one, low correlations are assumed; and if $\nu = 1$, no prior knowledge of the correlation is assumed. Here, ν is modeled as an exponential distribution with an expected value of one.

The equations (17) show a summary of all prior assumptions. Here, $\mathcal{N}^{\mathcal{T}}$ denotes the truncated Gaussian, where the hyperparameter a_k, b_k, and the support S_k are chosen such that the properties satisfy Table 2 for $k = 1, 2, 3, 4$. While w_j^2 represents the variances calculated in [16] for $j = 1, \ldots, 21$.

$$\begin{aligned} y_i|\theta &\sim \mathcal{N}_{21}(\mathrm{M}_i(\phi), \Sigma), \\ \theta &= (\phi, \Sigma), \\ \phi_k &\sim \mathcal{N}^{\mathcal{T}}(a_k, b_k, S_k), \\ \Sigma &= D\Omega D, \\ D &= \mathrm{diag}(\sigma_1, \ldots, \sigma_{21}), \\ \sigma_j^2 &\sim \mathrm{Exp}(1/w_j^2), \\ \Omega|\nu &\sim \mathrm{LKJ}(\nu), \\ \nu &\sim \mathrm{Exp}(1). \end{aligned} \tag{17}$$

4.3 Posterior sampling

The software STAN [18, 19] is used to derive the posteriors. For the sampling procedure, the No-U-Turn Sampler (NUTS) is applied, which allows random numbers that are distributed like the posteriors to be drawn without calculating them analytically. The notation, $\theta^{(s)}$ represents the sample number s for $s = 1, \ldots, S$. For the following steps, $S = 4000$ samples are utilized for each parameter.

4.4 Posterior results

A summary of the results of the physical fit parameters ϕ is shown in Table 3. While c_L, γ, and η_int are credible, C deviates quite strongly from what is expected.

Therefore, a second model variant under the condition that C = 0.91, and $\eta_\mathrm{int} = 0.01$, which are the values according to ISO 12354-1, was applied. In this case, a shift of the model curve is required. Figure 1 compares these models by visualizing $\frac{1}{S}\sum_{s=1}^{S} \mathrm{M}_i(\phi^{(s)})$. As the model curves are generated for each wall, the thickness of the curves reflects the influence of the wall properties. The Figures 2, 3, 4, and 5 compare the posterior samples between these two model variants with each other and with sampling from the prior densities.

For the future steps, the focus is on the model for which η_int and C are considered as non-fixed parameters since this has the better quality according to measures such as leave-one-out cross validation (LOO-CV) and WAIC [20]. The model with fixed parameters η_int and C only serves as a comparison.

The results of the standard deviations and correlations are summarized in Figures 6 and 7. For the standard deviations, both the median curve and the corresponding quantile ranges are shown. The values are also compared with the calculations according to Wittstock. The correlation was averaged across all sampled matrices. It can be seen that the correlations in the one-third octave bands below the critical frequency ($\approx$ 240 Hz) are rather weak, whereas the one-third octave bands above correlate rather strongly. An explanation might be that below the critical frequency the sound transmission is dominated by the forced transmission. The individual structural behavior does not play a significant role.

Table 3. Posterior summary of fit parameters

Quantiles	η_int	C	c_L	γ
2.5%	0.005	3.44	1019	0.57
25%	0.007	3.91	1047	0.60
50%	0.009	4.16	1061	0.61
75%	0.012	4.41	1075	0.64
97.5%	0.020	4.85	1100	0.68

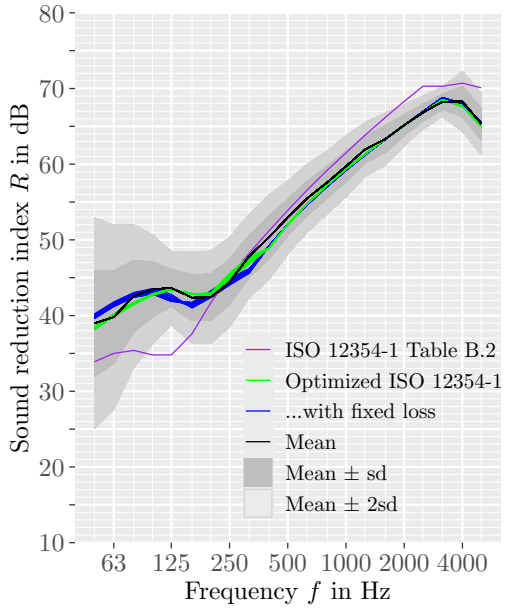

Figure 1. Model comparisons

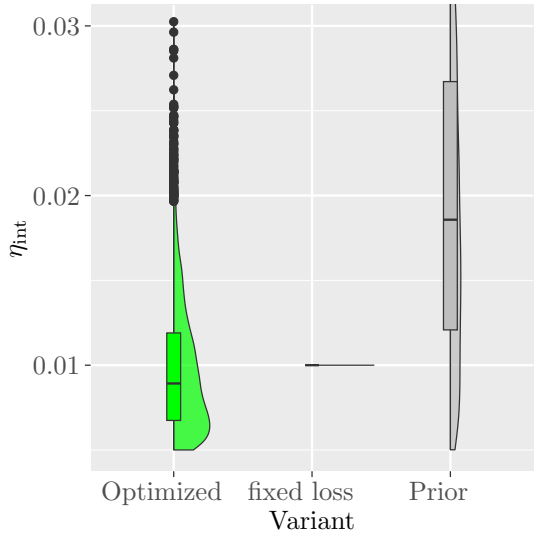

Figure 2. Posterior sample comparison of η_{int}

5. ANALYSIS OF R_{w}

The optimized model discussed is applied to simulate the sound reduction index. Let $W(t)$ be the properties of a Ca-Si wall with a thickness of t meter and the rest as in the data (see Table 1). As before, the notation $\mathrm{M}_{W(t)}(\phi)$ is used for the sound reduction index of a wall with the properties $W(t)$ as a function of the parameters ϕ.

The difference between the model and the measurement curve is simulated by drawing from a $\mathcal{N}_{21}(0, \Sigma^{(s)})$ distribution for each s. These 4000 simulated vectors of differences are each added to the corresponding $\mathrm{M}_{W(t)}(\phi^{(s)})$. This procedure is carried out in steps of one cm with wall thicknesses t from 0.18 meters to 0.36 meters. This results in 4000 simulated shapes of the sound reduction index R for each wall thickness, which can then be used to calculate the weighted sound reduction index R_{w} according to ISO 717-1 [21]. Note that by using all 4000 draws, the distribution and thus the estimation uncertainties of the parameters are taken into account.

The results are shown in Figure 8. The blue points in this figure show a comparison with the model variant in which the internal loss factor η_{int} and the boundary loss factor C are fixed.

These simulated values of the weighted sound reduction index R_{w} can then be utilized to estimate the proba-

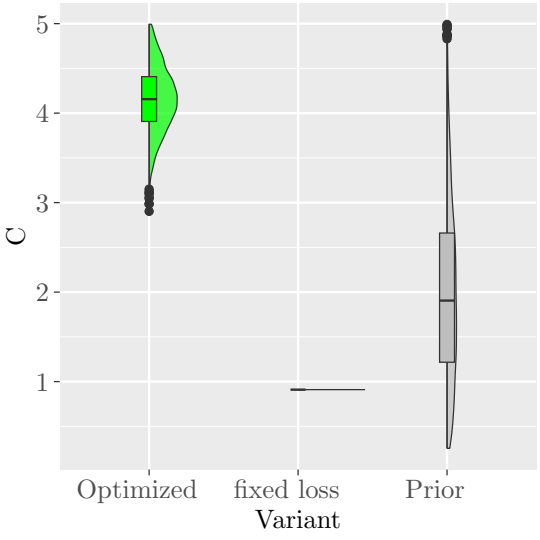

Figure 3. Posterior sample comparison of C

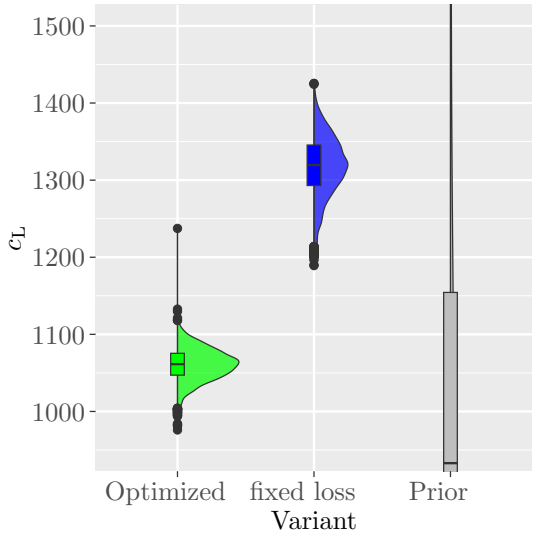

Figure 4. Posterior sample comparison of c_L

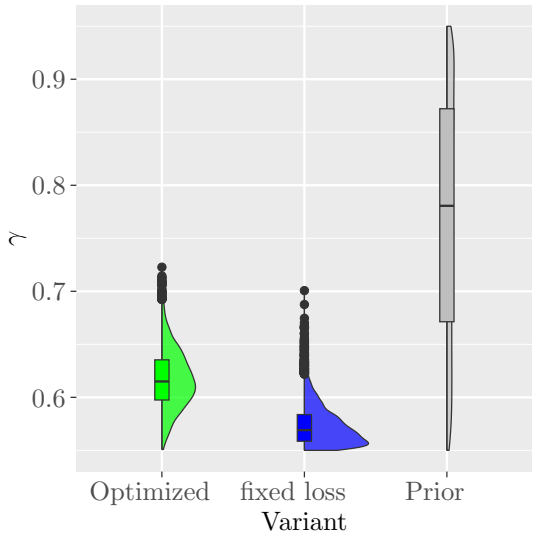

Figure 5. Posterior sample comparison of γ

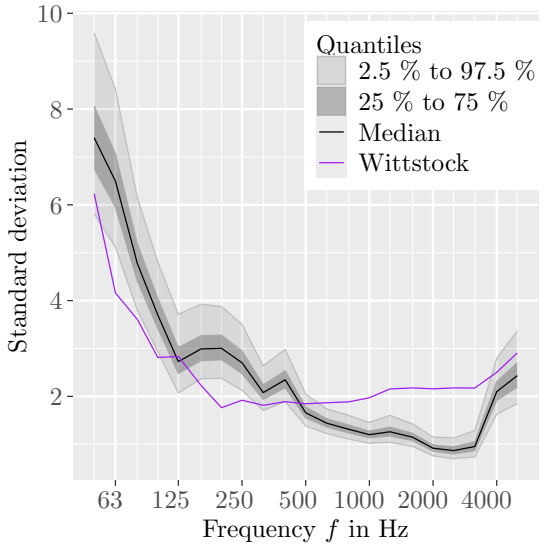

Figure 6. Estimated posterior distribution of the standard deviation in comparison with the calculations according to Wittstock

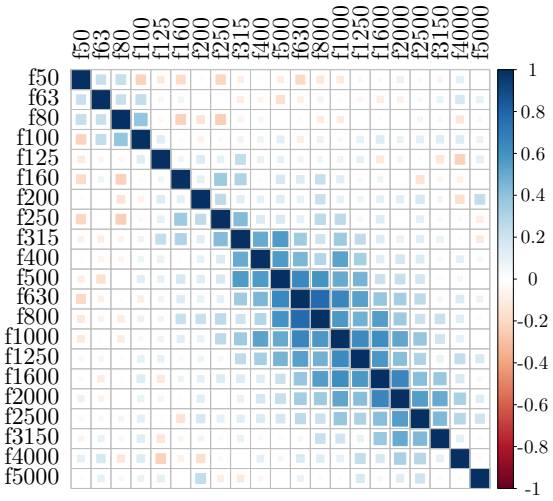

Figure 7. Averaged correlations

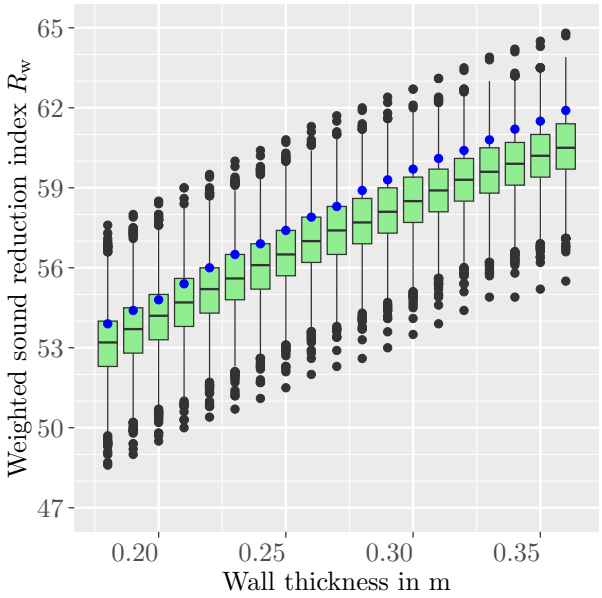

Figure 8. Simulated R_w values

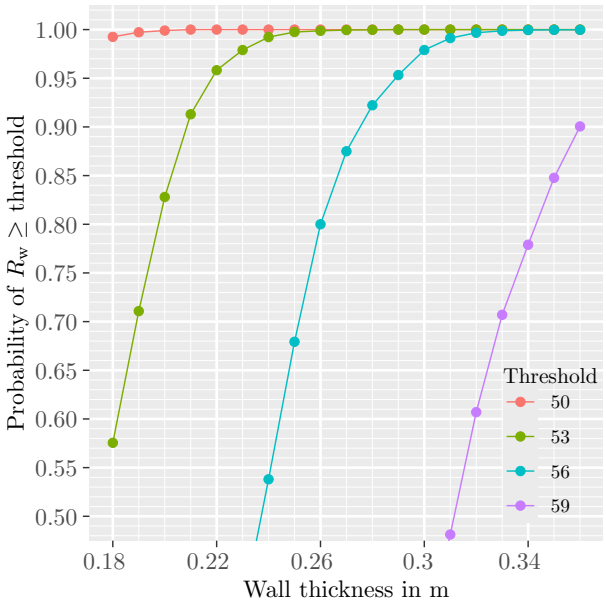

Figure 9. Estimated probability of R_w exceeding a threshold depending on the wall thickness

bility of specified threshold values being exceeded using relative frequencies. These results for probabilities of at least 0.5 are shown in Figure 9.

On the one hand, it can be seen that, according to this analysis, very high requirements of at least 59 dB need correspondingly thick walls of 36 cm to be fulfilled with a probability of about 90 %. On the other hand, low requirements of 50 dB are almost always met also with 18 cm walls.

Assuming 53 dB is set as the threshold value, the question arises as to the probability with which this should be reached. If this is to be fulfilled in at least 90 % of cases, then a thickness of 21 cm is sufficient, and for 95 % it should be 22 cm.

6. DISCUSSION

In this work, the physical model according to ISO 12354-1 was first adapted and then optimized using Bayesian methods. With the help of simulations based on the physical model and probability assumptions, sound reduction index R curves of Ca-Si walls at different thicknesses were simulated. These simulated curves were in turn taken to provide information on the distribution of the weighted sound reduction index R_w depending on the wall thickness.

However, it should be noted that the accuracy of the physical model cannot be verified for wall thicknesses other than 25 cm, but since the model itself is strongly based on the surface area mass, it is credible that the model still fits.

This procedure should therefore be repeated on the basis of other data. In addition to calcium silicate walls with different wall thicknesses, other materials such as reinforced concrete walls or lightweight concrete are also conceivable. In addition, further physical models for the sound reduction index R are to be utilized as a basis, in particular model variants based on the in-situ case.

Overall, it can be stated that this approach provides promising results, but further data and steps for validation are still necessary. However, the procedure itself remains identical regardless of the chosen physical model behind or the exact nature of the data.

7. ACKNOWLEDGEMENTS

We would like to thank the *Physikalisch-Technische Bundesanstalt* for providing the data from the round-robin test. In particular, Mr. Wittstock, who also provided us with his calculations for the one-third-band standard devi-

ations discussed in [16].
Furthermore we would like to acknowledge the funding of the research by the *Bavarian State Ministry of Education, Culture, Science and Arts*.

8. REFERENCES

[1] *Proceedings of Forum Acusticum 2023*, 2023.

[2] Deutsche Gesellschaft für Akustik e.V., ed., *Fortschritte der Akustik - DAGA*, 2024.

[3] Deutsche Gesellschaft für Akustik e.V., ed., *Fortschritte der Akustik - DAGA*, 2023.

[4] DIN EN ISO 12354-1:2017-11, "Bauakustik – berechnung der akustischen eigenschaften von gebäuden aus den bauteileigenschaften: Teil 1: Luftschalldämmung zwischen räumen."

[5] Deutsche Gesellschaft für Akustik e.V., ed., *DAS/DAGA 2025 - 51st Annual Meeting on Acoustics*, 2025.

[6] W. Weise and V. Wittstock, "Using round robin test results for the accreditation of laboratories in the field of building acoustics in germany," *Building Acoustics*, no. 12, pp. 189–206, 2005.

[7] DIN EN ISO 10140-5:2021-09, "DIN EN ISO 10140-5:2021-09, Akustik- Messung der Schalldämmung von Bauteilen im Prüfstand- Teil 5: Anforderungen an Prüfstände und Prüfeinrichtungen (ISO 10140-5:2021); Deutsche Fassung EN ISO 10140-5:2021."

[8] W. M. Bolstad and J. M. Curran, *Introduction to Bayesian statistics*. THEi Wiley ebooks, Hoboken, NJ: Wiley, third edition ed., 2017.

[9] A. Gelman, J. B. Carlin, H. S. Stern, and D. B. Rubin, *Bayesian data analysis*. Texts in statistical science series, Boca Raton, Fla. u.a.: Chapman & Hall/CRC, 2. ed. ed., 2004.

[10] J. Wakefield, *Bayesian and Frequentist Regression Methods*. Springer Series in Statistics, New York, NY: Springer New York, 2013.

[11] E. T. Jaynes, "Information theory and statistical mechanics," *Phys. Rev.*, vol. 106, pp. 620–630, May 1957.

[12] E. T. Jaynes, "Information theory and statistical mechanics. ii," *Phys. Rev.*, vol. 108, pp. 171–190, Oct 1957.

[13] D. Dowson and A. Wragg, "Maximum-entropy distributions having prescribed first and second moments (corresp.)," *IEEE Transactions on Information Theory*, vol. 19, no. 5, pp. 689–693, 1973.

[14] E. T. Jaynes, *Probability Theory - The Logic of Science*. Cambridge: Cambridge University Press, 2003.

[15] P. C. Gregory, *Bayesian logical data analysis for the physical sciences: A comparative approach with Mathematica support*. Cambridge University Press, 2005.

[16] V. Wittstock, "Determination of measurement uncertainties in building acoustics by interlaboratory tests. part 1: Airborne sound insulation," *Acta Acustica united with Acustica*, vol. 101, no. 1, pp. 88–98, 2015.

[17] D. Lewandowski, D. Kurowicka, and H. Joe, "Generating random correlation matrices based on vines and extended onion method," *Journal of Multivariate Analysis*, vol. 100, no. 9, pp. 1989–2001, 2009.

[18] Stan Development Team, "Stan: Stan reference manual," 2024.

[19] Stan Development Team, "RStan: the R interface to Stan," 2024. R package version 2.32.6.

[20] A. Vehtari, A. Gelman, and J. Gabry, "Practical bayesian model evaluation using leave-one-out cross-validation and waic," *Statistics and Computing*, vol. 27, no. 5, pp. 1413–1432, 2017.

[21] DIN EN ISO 717-1:2021-05, "Akustik - bewertung der schalldämmung in gebäuden und von bauteilen: Teil1: Luftschalldämmung," 2021.